Adipose Triglyceride Lipase Is a Key Lipase for the Mobilization of Lipid Droplets in Human β-Cells and Critical for the Maintenance of Syntaxin 1a Levels in β-Cells

Siming Liu,[1,2] Joseph A. Promes,[1,2] Mikako Harata,[1,2] Akansha Mishra,[1,2] Samuel B. Stephens,[1,2] Eric B. Taylor,[1,2] Anthony J. Burand Jr.,[2,3] William I. Sivitz,[1,2] Brian D. Fink,[1,2] James A. Ankrum,[2,3] and Yumi Imai[1,2]

Diabetes 2020;69:1178–1192 | https://doi.org/10.2337/db19-0951

Lipid droplets (LDs) are frequently increased when excessive lipid accumulation leads to cellular dysfunction. Distinct from mouse β-cells, LDs are prominent in human β-cells. However, the regulation of LD mobilization (lipolysis) in human β-cells remains unclear. We found that glucose increases lipolysis in nondiabetic human islets but not in islets in patients with type 2 diabetes (T2D), indicating dysregulation of lipolysis in T2D islets. Silencing adipose triglyceride lipase (ATGL) in human pseudoislets with shRNA targeting ATGL (shATGL) increased triglycerides (TGs) and the number and size of LDs, indicating that ATGL is the principal lipase in human β-cells. In shATGL pseudoislets, biphasic glucose-stimulated insulin secretion (GSIS), and insulin secretion to 3-isobutyl-1-methylxanthine and KCl were all reduced without altering oxygen consumption rate compared with scramble control. Like human islets, INS1 cells showed visible LDs, glucose-responsive lipolysis, and impairment of GSIS after ATGL silencing. ATGL-deficient INS1 cells and human pseudoislets showed reduced SNARE protein syntaxin 1a (STX1A), a key SNARE component. Proteasomal degradation of Stx1a was accelerated likely through reduced palmitoylation in ATGL-deficient INS1 cells. Therefore, ATGL is responsible for LD mobilization in human β-cells and supports insulin secretion by stabilizing STX1A. The dysregulated lipolysis may contribute to LD accumulation and β-cell dysfunction in T2D islets.

Overnutrition is the major risk factor of type 2 diabetes (T2D) and causes lipid accumulation in insulin target tissues resulting in insulin resistance by provoking inflammation and other stress responses (1). Excessive lipid accumulation is also blamed for β-cell dysfunction in T2D (2), the other key pathology of T2D (3). Although lipid accumulation in nonadipocytes, including hepatocytes and myocytes, manifests as increased lipid droplets (LDs) (4), the presence of LDs in β-cells has been underappreciated due to difficulty demonstrating LDs in mouse β-cells (5–7). Recently, LD and LD-associated proteins were shown to be increased in human β-cells under fatty acid (FA) loading (5), on high-fat diet (HFD) (6), and in T2D (8,9), indicating that LD accumulation is a hallmark of nutritional overload in human β-cells. However, little is currently known regarding factors that drive LD accumulation and mobilization (lipolysis) in human β-cells.

LDs consist of a core of neutral lipids covered by a phospholipid monolayer that is studded with proteins that regulate lipid metabolism and the interaction of LDs with other organelles (4,10). Although classically viewed as a static storage organelle, LDs are now recognized to actively produce lipid metabolites and interact dynamically with organelles, including mitochondria and nuclei, to coordinate intracellular lipid metabolism in a wide range of cells (10,11). Our previous studies showed that the LD proteins perilipin (PLIN) 2 and PLIN5 were dynamically upregulated in response to nutritional influx in β-cells indicating that these LDs functioned as active organelle (5,7). Since LD accumulation in β-cells, as occurs with overnutrition or T2D, is likely due to an imbalance between LD formation and mobilization, it is important to improve our understanding of both processes.

[1]Department of Internal Medicine, Carver College of Medicine, University of Iowa, Iowa City, IA
[2]Fraternal Order of Eagles Diabetes Research Center, University of Iowa, Iowa City, IA
[3]Roy J. Carver Department of Biomedical Engineering, University of Iowa, Iowa City, IA

Corresponding author: Yumi Imai, yumi-imai@uiowa.edu

Received 20 September 2019 and accepted 28 February 2020

This article contains supplementary material online at https://diabetes.diabetesjournals.org/lookup/suppl/doi:10.2337/db19-0951/-/DC1.

LD mobilization by lipolysis is initiated by adipose triglyceride lipase (ATGL, aka PNPLA2) in most cells and produces *sn*-1,3 diacylglycerides, *sn*-2,3 diacylglycerides, *sn*-1 or 2-monoaclglycerides (MAG), glycerol, and FA after stepwise removal of FA from TGs (10,11). In addition to its potential role in determining the balance of LD accumulation during overnutrition, there has been a strong interest in lipolysis in β-cells historically (12,13). Lipolysis is proposed to generate metabolites that support glucose-stimulated insulin secretion (GSIS) based on acute reduction of GSIS in rat islets and β-cell lines by the pan lipase inhibitor, orlistat (12,14). Two studies of β-cell–specific ATGL knockout (KO) mice proposed that ATGL deficiency blunts insulin secretion through two distinct mechanisms (15,16). Tang et al. (15) demonstrated that RIP-Cre–mediated ATGL deficiency impairs β-cell function through downregulation of peroxisome proliferator–activated receptor (PPAR) δ target genes leading to mitochondrial dysfunction suggesting that FAs derived by lipolysis activate PPARδ in β-cells. Attané et al. (16) proposed that MIP-Cre–mediated ATGL deficiency blunts insulin secretion by reducing the production of 1-MAG that activates mammalian uncoordinated (MUNC) 13–1 to stimulate exocytosis (17). In the study by Attané et al., mitochondrial dysfunction was not observed in ATGL-deficient islets. At the same time, a role for MAG in GSIS is inconclusive since the pharmacological inhibition of MAG lipase reduced GSIS in INS1 cells and rat islets despite the increase in MAG (18). Collectively, the mechanism by which ATGL deficiency impairs insulin secretion remains inconclusive and has not been clarified in human β-cells.

In addition to the controversy regarding consequences of impaired lipolysis, the regulation of lipolysis in β-cells remains unclear. In β-cells, glucose is believed to increase lipolysis based on glycerol release measured in mouse (19) and rat islets (14,20). However, it was recently found that β-cells generate glycerol from glycerol 3-phosphate bypassing lipolysis (21). Surprisingly, there is little information regarding the regulation of lipolysis in pancreatic islets and β-cells if one excludes studies that used glycerol release as a marker of lipolysis (14). Moreover, it is unknown whether glucose regulates lipolysis in human islets.

Here, we addressed the roles of lipolysis in human islets using TG reduction in the presence of Triacsin C to measure lipolysis. We report that glucose increased lipolysis in human islets from donors without diabetes but not in human islets from T2D donors. We also found that downregulation of ATGL increased TG and caused LD accumulation confirming ATGL as a key lipase in human β-cells. Additionally, ATGL deficiency impaired insulin secretion in human pseudoislets providing evidence that lipolysis maintains insulin secretion in a human β-cell model. The impairment in insulin secretion in ATGL-deficient human pseudoislets and INS1 cells was associated with the reduction of SNARE protein syntaxin 1a (STX1A) (22) revealing a previously unidentified target of ATGL.

RESEARCH DESIGN AND METHODS

Human Islets

Human islets from donors without diabetes and donors with T2D (Supplementary Table 1) were cultured in CMRL1066 containing 1% human serum albumin, 1% Pen-Strep, and 1% L-glutamate for overnight at 37°C and 5% CO_2 prior to analyses. The institutional review board at University of Iowa determined this to be a nonhuman study.

Mouse Studies

Experiments were approved by the University of Iowa Institutional Animal Care and Use Committee. C57Bl/6NJ (Bl6) mice were from The Jackson Laboratory. $ATGL^{fl/fl}$ (024278; The Jackson Laboratory) and $INS1^{cre}$ (026801; The Jackson Laboratory) were crossed to create β-cell–specific ATGL-deficient mice ($INS1^{Cre/+}ATGL^{fl/fl}$, ATGL KO) and $INS1^{+/+}ATGL^{fl/fl}$ (wild type [WT]) as littermate controls. Mice had free access to regular rodent chow. To carry out the glucose tolerance test, 2-month-old male ATGL KO and WT mice were fasted overnight and given 1.5 g/kg body weight glucose intraperitoneally followed by measurement of tail blood glucose via a hand-held glucometer at the indicated time points. Islets were isolated from 12- to 16-week-old male mice by Ficoll density gradient centrifugation of collagenase-digested pancreas (7) and cultured in RPMI1640 with 10% FBS and 1% Pen-Strep (mouse islet medium).

INS1 Cells

The 823/13 INS1 cells (INS1 cells, a kind gift from Dr. C. Newgard of Duke University) were maintained in RPMI1640 supplemented with 10% FBS, 10 mmol/L HEPES, 2 mmol/L L-glutamine, 1 mmol/L sodium pyruvate, 50 μmol/L β-mercaptoethanol, and penicillin + streptomycin (INS1 medium) (23). Cells were used within 12 passages from the original vial.

Bodipy C12 Labeling of LD and Confocal Microscopy

INS1 cells plated on a cover glass coated with HTB-9 cell–derived matrix (23) were cultured in INS1 medium containing 0.4 mmol/L oleic acid (OA) overnight. Human and mouse islets cultured in respective medium containing 0.4 mmol/L OA overnight were plated on confocal dishes after dispersion by Accutase (MilliporeSigma, St Louis, MO). INS1 cells and islets were maintained in medium containing 2 μmol/L Bodipy 558/568 C_{12} (Bodipy C12; Molecular Probes) for an additional 24 h and immunostained with insulin antibody (Supplementary Table 2) or 2 μmol/L Bodipy 493/503 (Bodipy 493, Molecular Probes) as published (5) to image LD by a Zeiss LSM710 microscope.

Lipolysis Assay

INS1 cells in 12-well plates, 50 mouse islets, 50 islet equivalents of human islets, or 120–150 human pseudoislets were preincubated in Krebs-Ringer bicarbonate (KRB)

buffer with 2 mmol/L glucose and 10 μmol/L Triacsin C for 60 min, and the time 0 group was harvested in radioimmunoprecipitation assay buffer with protease inhibitors. Then, cells or islets were treated with 2 mmol/L or 16.8 mmol/L glucose plus 10 μmol/L Triacsin C for 90 min with addition of atglistatin in some INS1 cells. TGs extracted from the cell or islet lysate by Folch buffer as published (7) was quantitated by Infinity Reagents (Fisher Scientific) and corrected for mg protein. Triacsin C blocks the activation of FAs to form Acyl-CoA and prevents the synthesis of new TGs including re-esterification of FAs released by lipolysis (24). Thus, lipolysis can be calculated as the reduction of TGs during the observation period (90 min in the current study).

Downregulation of ATGL and STX1A

Human pseudoislets transduced by lentivirus carrying scramble (scr) shRNA ([scr], CCTAAGGTTAAGTCGCCCTCG) or shRNA targeting ATGL ([shATGL], CCTGCCACTCTATGAGCTTAA, TRCN0000222744 from Genetic Perturbation Platform [https://portals.broadinstitute.org/gpp/public]) under U6 promoters were created at 500 cell/well in AggreWell 400 (STEMCELL Technology) as published (25). In brief, human islets were incubated with Accutase at 37°C for 5 min, pipetted 15 times through a 1 mL tip, digested for an additional 4 min at 37°C, and passed through a 40-μm strainer to make a single-cell suspension in 10% FBS CMRL (human islet medium). A 40 transducing unit/cell of lentivirus was added to 6×10^5 single islet cells in a total of 1 mL of human islet medium followed by incubation at 37°C for 1 h with occasional gentle mixing. Then, the single-cell suspension with virus was adjusted to 2 mL in 10% FBS CMRL, transferred to one well of the AggreWell 400, and centrifuged at 100*g* for 3 min at room temperature to capture cells in microwells. Thereafter, cells were cultured in human islet medium for 7 days. The second shRNA targeting ATGL (shATGL2, GCCACTCTATGAGCTTAAGAA, TRCN0000078196 from Genetic Perturbation Platform) was also used where indicated. A 2×10^5/24 wells of INS1 cells plated the day before were transfected with 15 nmol/L each of siRNA targeting ATGL (siATGL, rn.Ri.Pnpla2.13.2 and rn.Ri.Pnpla2.13.3 from IDT) or 30 nmol/L of nontargeting RNA (scr, IDT) using DharmaFect (Dharmacon) as published (23) and harvested 72 h later. To inhibit proteasome, 10 μmol/L MG132 was added 8 h before harvest. To downregulate *Stx1a* expression, INS1 cells were transfected with either siRNA rn.Ri.Stx1a.13.3 or rn.Ri.Stx1a.13.2 (both from IDT) at 30 nmol/L using scr siRNA (IDT) as a control.

Imaris Analysis of LDs in Human Islets

The 200 human pseudoislets created in AggreWell were dispersed, plated on confocal dishes, and stained for insulin and Bodipy 493 as above. Nine fields containing insulin-positive cells were randomly chosen, and Z-stack images of the entire *z*-axis of each insulin-positive cell were obtain by a Zeiss LSM710 microscope and three-dimensional reconstruction was performed using Imaris software (Bitplane) with measurement of integrated fluorescent intensity and volume of each LD in a surpass mode.

Transmission Electron Microscopy

Pseudoislets were fixed with 2.5% glutaraldehyde in 0.1 mol/L sodium cacodylate buffer (pH 7.4) overnight at 4°C, then postfixed with 1% Osmium tetroxide for 1 h. Following serial alcohol dehydration (50%, 75%, 95%, and 100%), the samples were embedded in epon 12. The 70-nm sections poststained with uranyl acetate and lead citrate were examined with a JEOL 1230 transmission electron microscope (EM).

Quantitative PCR

RNA isolated from islets using TRIzol reagent (Thermo Fisher) or from INS1 cells using RNeasy kit (Qiagen) was reverse-transcribed into cDNA using Superscript IV VILO Master Mix (Thermo Fisher). Quantitative PCR (qPCR) used TaqMan commercial primers (Applied Biosystems). Cycle threshold value (C_T) for each gene was obtained using Applied Biosystems 7900HT and the expression levels of each gene was calculated as $2^{-(\Delta\Delta\ C_T)}$ that is a power of 2 of the difference between C_T value of a gene of interest and *PPIB* (26). C_T for *PPIB* did not differ between groups treated with scr and siATGL/shATGL in both human pseudoislets and INS1 cells when C_T significantly increased with siATGL/shATGL (Supplementary Fig. 1*A*, *B*, *D*, and *E*). $\Delta\Delta$ C_T between *PPIB* and β-Actin (*ACTB*) did not differ between scr- and siATGL/shATGL-treated human pseudoislets and INS1 cells either (Supplementary Fig. 1*C* and *F*), indicating that *PPIB* expression was not affected by siATGL/shATGL and served as an appropriate housekeeping gene.

Insulin Secretion and Oxygen Consumption Rate

Pseudoislets were perifused at 0.12 mL/min in KRB buffer containing 2.8 mmol/L glucose for 52 min followed by 16.7 mmol/L glucose, 100 μmol/L 3-isobutyl-1-methylxanthine (IBMX) in 8.3 mmol/L glucose, or 30 mmol/L KCl in 2.8 mmol/L glucose using a Perifusion System (Biorep Technologies) as published (27). The stimulation index (SI) is defined as a ratio of average insulin secretion during 16.7 mmol/L glucose to that at 2.8 mmol/L glucose. For INS1 cells or mouse islets, insulin secreted into the KRB buffer at the indicated concentration of glucose during 1 h was measured after 1 h preincubation in glucose-free KRB buffer. Ten size-matched islets in triplicates per condition were used for mouse islets. Insulin was extracted from islets or INS1 cells by acidified ethanol as published (7). A stock solution of 100 mmol/L 1-palmitoyl-glycerol (MilliporeSigma), a 1-MAG species previously shown to augment GSIS (17), was prepared in DMSO and added at a final concentration of 0.1 mmol/L for the duration indicated in the figure legends. DMSO alone was used as a vehicle control. Insulin was measured using human STELLUX ELISA kit (ALPCO) or mouse ultrasensitive insulin ELISA

kit (ALPCO). The oxygen consumption rate (OCR) was obtained using an XF24 Seahorse extracellular flux analyzer (Seahorse Bioscience) from 150 islets/well of human pseudoislets as published (28).

Immunoblotting

INS1 cell or islet lysates in radioimmunoprecipitation assay buffer were separated on 4–12% Bis-Tris Gel and transferred to polyvinylidene fluoride membranes. Membranes were incubated with primary antibodies followed by secondary antibodies (Supplementary Table 2) and visualized by SuperSignal West Pico chemiluminescent detection system as published (5). Densitometric analyses were performed by ImageJ software (ImageJ.nih.gov). GAPDH and β-tubulin expression was similar between the control group and ATGL-deficient human pseudoislets and INS1 cells supporting the use of GAPDH as a loading control (Supplementary Fig. 1*G* and *H*).

Acyl-PeGyl Exchange Gel Shift Assay

Acyl-PeGyl exchange gel shift (APEGS) assay of scr or siATGL transfected INS1 cell followed a published protocol (29). In brief, 190 μg of protein lysate reduced by 25 mmol/L Tris(2-carboxyethyl)phosphine was treated with 50 mmol/L N-ethylmaleimide to block free thiols. Then, lysates were mixed with 1 mol/L hydroxylamine that cleaves s-palmitoylated FA from cysteine or with 1 mol/L Tris, pH 7 (negative control). Newly exposed free thiols were labeled with 20 mmol/L of maleimide-conjugated methoxy polyethylene glycol (mPEG-2k, SUNBRIGHT ME-020MA; NOF corporation).

Statistics

Data are presented as mean ± SEM. Numeric differences between the two groups were assessed with Student *t* tests with Welch correction when indicated. A one-way ANOVA with Dunnett test was performed for data consisting of three groups, and a two-way ANOVA test was performed to assess perifusion and the glucose tolerance test. All data analyses were carried out using Prism 8 (GraphPad). A P value of <0.05 was considered significant.

Data and Resource Availability

The data sets generated during and/or analyzed during the current study are available from the corresponding author upon reasonable request.

RESULTS

Glucose Increases Lipolysis in Human Islets and INS1 Cells but Not in Mouse Islets

Because LD size reported in β-cells differs depending on species (5,6,9,30), LDs actively formed during culture in human β-cells, INS1 cells, and mouse β-cells were compared in parallel by Bodipy C12, a bioortholog of C16 FA that preferentially labels TGs (31) (Fig. 1*A*–*C*). Human β-cells and INS1 cells, but not mouse β-cells, formed visible LDs under confocal microscopic observation (Fig. 1*A*–*C*). Visibility of LDs did not correlate with TG contents since TG contents of mouse and human islets were comparable and higher than in INS1 cells (Fig. 1*D*). There was a trend toward increased TG content in human T2D islets compared with islets from donors without diabetes (Table 1) in agreement with a reported increase in lipid accumulation in T2D islets (8,9) (Fig. 1*D*). When lipolysis was measured as the reduction of TGs under the inhibition of TG synthesis by triacsin C, 16.8 mmol/L of glucose increased lipolysis compared with 2 mmol/L of glucose in human islets from donors without diabetes. This did not occur in T2D islets, suggesting that dysregulated lipolysis might contribute to TG accumulation in T2D (Fig. 1*E* and *F*). The reduction in glucose stimulated lipolysis in T2D islets was not due to the reduction of ATGL protein (Fig. 1*G*). Glucose increased lipolysis by 2.1-fold in INS1 cells, an effect that was blocked by the rodent-specific ATGL inhibitor atiglistatin (32), indicating that ATGL is primarily responsible for lipolysis in INS1 cells (Fig. 1*H*). High glucose mobilized >30% of TGs over 90 min in both human islets from donors without diabetes and INS1 cells, indicating high TG turn over in the presence of glucose. In contrast, mouse islets showed high rate of lipolysis at low glucose that did not increase further at high glucose (Fig. 1*I*).

ATGL Deficiency Increases LD in Human Pseudoislets

While the reduction of lipolysis by atglistatin indicated ATGL is the key TG lipase in INS1 cells, the lack of a human-specific ATGL inhibitor prohibited similar pharmacological studies in human islets (32). The pan lipase inhibitor, orlistat, is relatively specific for human ATGL, but also inhibits FA synthase (33,34). Furthermore, to understand the consequence of dysregulated TG lipolysis in human T2D islets, the impact of continuous suppression of LD mobilization in human islets needs to be addressed. Previous studies by ourselves and others have demonstrated that human pseudoislets maintain dynamic insulin secretion during culture (27), show similar expression of markers of cell type and β-cell function by qPCR (27), and have a distribution of β-cells and non-β-cells similar to original human islets (35). *ATGL* expression tested by qPCR was comparable between human islets without dispersion and pseudoislets as well (Supplementary Fig. 1*I*). Thus, we created human pseudoislets in which ATGL was efficiently reduced both at mRNA (Fig. 2*A*) ($P < 0.05$) and protein levels (Fig. 2*B*) ($P < 0.05$). We did not observe compensatory increases in mRNA coding *LIPE* or the ATGL activator, *ABHD5* (Fig. 2*C*). For mRNA coding genes involved in TG synthesis and LD proteins, shATGL islets showed ~1.7-fold increase of *DGAT2* and slightly reduced PLIN5 compared with control, while *DGAT1*, *PLIN2*, and *PLIN3* were unchanged (Fig. 2*C* and Supplementary Fig. 2*A* and *B*). Interestingly, *CPT2* and *ACDVL*, mitochondrial genes downregulated in islets from RIP-Cre β-cell–specific ATGL-deficient mice (15), were not altered in ATGL-deficient human islets (Fig. 2*C*). PLIN2, the major LD protein in

human islets (5,7), was significantly increased in shATGL islets by immunoblot (Fig. 2*D*) but not at the mRNA level (Fig. 2*C*), which may reflect posttranslational stabilization typically seen when neutral lipid storage is increased (36). As expected, since ATGL is a TG lipase and in agreement with the increase in PLIN2, TG contents were increased in shATGL-treated human pseudoislets (Fig. 2*E*). When the change in lipolysis by high glucose is measured as in

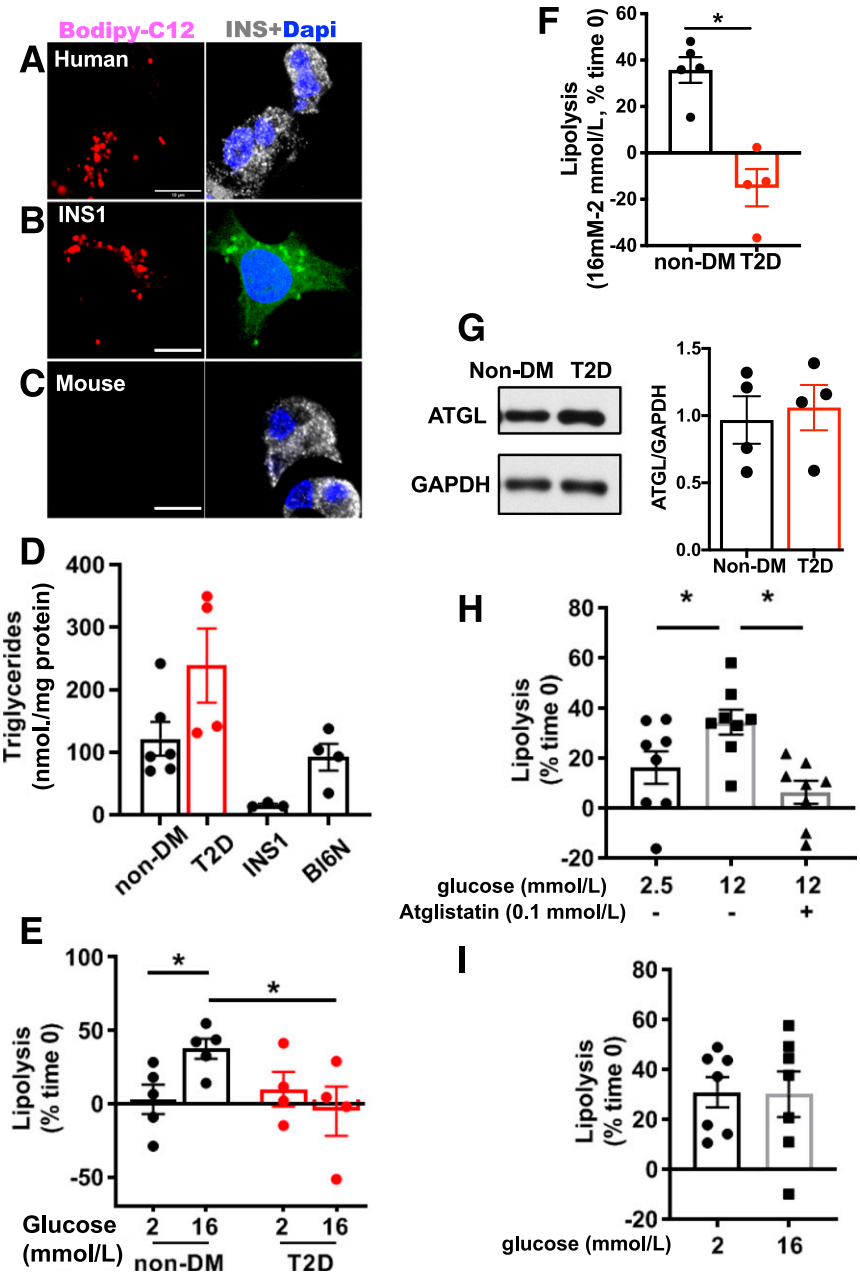

Figure 1—Human islets and INS1 cells, but not mouse islets, showed distinct LD and increased lipolysis in response to glucose. *A–C*: Confocal images of human β-cells (*A*), INS1 cells (*B*), and β-cells from BI6NJ (BI6N) mouse islets (*C*) incubated with 0.4 mmol/L OA + 2 μmol/L Bodipy C12 overnight as in RESEARCH DESIGN AND METHODS. Human and mouse β-cells were identified by anti-insulin antibody (white) while INS1 cells were instead stained with Bodipy 493 (green). DAPI in blue. Scale bars = 10 μm. *D*: TG contents of INS1 cells, human islets from donors without diabetes (non-DM), and donors with T2D, and from BI6N. $n = 5$ for non-DM, $n = 4$ for T2D, $n = 3$ for INS1 cells, and $n = 4$ for BI6N. *E*: Lipolysis measured in human islets from non-DM and T2D. Data represent TG contents per mg protein at time 0 as 100%. $n = 4$–5 donors. *F*: Data from *E* are expressed as the increase in lipolysis in response to glucose for non-DM and T2D. $n = 4$–5 donors. *G*: Representative immunoblot comparing ATGL expression in human islets from non-DM and T2D donors. GAPDH served as loading control and densitometry data are expressed as ATGL/GAPDH. $n = 4$. *H*: Lipolysis measured as in *E* in INS1 cells at indicated concentration of glucose in the presence and absence of atglistatin. $n = 8$. *I*: Lipolysis measured as in *E* in BI6N islets. $n = 7$. All data are mean ± SEM. *$P < 0.05$ by Student *t* test.

Table 1—Human islet donor information

	n	Age (year)	Sex (male/female)	BMI (kg/m^2)	HbA_{1c} (%)
Without diabetes	5	47.4 ± 8.4 (18–69)	3/2	26.1 ± 2.3 (19–33.3)	5.2 ± 0.2 (4.7–5.7)
With T2D	4	50.3 ± 6.1 (34–63)	2/2	32.5 ± 1.3 (29.5–35.4)	9.3 ± 1.0 (7.3–11.9)

Data are presented as mean ± SEM (range).

Fig. 1*F*, glucose increased lipolysis in the scr control group indicating that human pseudoislets maintain lipolytic response to glucose as in human islets from donors without diabetes (Fig. 2*F*). In contrast, the response to glucose was significantly blunted in shATGL islets suggesting that ATGL plays a key role in lipolysis in human islet cells (Fig. 2*F*). ATGL-deficient human β-cells showed prominent LDs by EM and confocal microscopy (Fig. 3*A* and *B*). The number of LDs per cell and volume distribution of LDs was shifted to higher values in the shATGL group compared with control in all three donor islets tested (Fig. 3*C* and *D*). As a result, the volume of all LDs combined in each cell was greatly increased in shATGL β-cells indicating that ATGL is essential to mobilize LDs in human β-cells (Fig. 3*E*).

ATGL-Deficient Human Pseudoislets Exhibit Impaired GSIS Without Mitochondrial Dysfunction

ATGL downregulated pseudoislets showed significantly reduced GSIS expressed as area under the curve (AUC) or SI (Fig. 4*A* and *B*). GSIS was also reduced when ATGL was downregulated using a separate shRNA (shATGL2) confirming the specificity of the finding (Supplementary Fig. 3*A* and *B*). Both first and second phases of GSIS were reduced in shATGL islets (Fig. 4*C* and *D*). Furthermore, insulin secretion to IBMX and KCl was lower in shATGL compared with control (Fig. 4*E–G*). Total insulin content was comparable between shATGL and scr islets (data not shown). Although there was a mild but significant increase in the expression of *GCG*, expression of *INS*, *PDX1*, and *MAFA* were unchanged in shATGL islets (Fig. 4*H* and Supplementary Fig. 2*C–E*). Markers for endoplasmic reticulum stress (*HSPA5*, *DDIT3*), cell stress (*TXNIP*), hypoxia (*HIF1a*), and inflammation (*CCL2*) were likewise not increased in shATGL islets (Fig. 4*I* and Supplementary Fig. 2*F* and *G*). We did not observe defects in OCR in response to glucose, oligomycin, FCCP, or rotenone/antimycin in ATGL-deficient human pseudoislets either (Fig. 4*J*). Along with unchanged *CPT2* and *ACDVL*, impaired insulin secretion in human ATGL-deficient islets occurred via a mechanism distinct from the reduced activation of PPARδ reported in RIP-Cre ATGL KO mice (15).

GSIS Is Blunted in ATGL-Deficient INS1 Cells but Not in ATGL KO Mouse Islets

The impairment in insulin secretion to various stimuli without mitochondrial dysfunction we observed in ATGL-deficient human pseudoislets agrees with reported phenotypes of INS1 cells after ATGL downregulation (37). We could reproduce blunting of GSIS in siATGL INS1 cells (Fig. 5*A–D*) along with normal OCR measured by Seahorse analyzer (data not shown). As 1-palmitoyl-glycerol, one of lipolytic metabolites, increases insulin secretion acutely by the activation of MUNC13–1 (17,38), we tested whether addition of 1-palmitoyl-glycerol for 1 h restores insulin secretion in ATGL-deficient INS1 cells (Fig. 5*E*). In agreement with previous reports in mouse islets (17,38), 1-palmitoyl-glycerol acutely increased GSIS in INS1 cells by 40–50% compared with glucose alone in both scr control and siATGL INS1 cells (Fig. 5*F* and Supplementary Fig. 3*C*). However, 1-palmitoyl-glycerol was not sufficient to restore insulin secretion in siATGL INS1 cells to the level of the scr control group indicating that an additional mechanism accounts for the reduction of GSIS in ATGL-deficient INS1 cells (Fig. 5*E*). A 24-h incubation with 1-palmitoyl-glycerol did not prevent the reduction of GSIS in ATGL-deficient INS1 cells (Fig. 5*G*) and did not augment GSIS in either scr- or siATGL-treated INS1 cells (Fig. 5*H*). When tested in two donor islets, 1-palmitoyl-glycerol was not sufficient to restore GSIS in ATGL-deficient human pseudoislets either (Supplementary Fig. 3*D*). Next, we analyzed islets from mice in which ATGL is downregulated in β-cells by INS1-Cre (39). We did not observe significant differences in body weight, fasting glucose, or glucose tolerance between INS1-Cre ATGL KO mice compared with WT littermates on regular chow (Fig. 6*A–C*). Unexpectedly, islets from β-cell–specific ATGL KO mice exhibited GSIS comparable to the control group despite clear reduction of ATGL protein in isolated islets (Fig. 6*D–F*) suggesting that effect of ATGL deficiency is similar in human islets and INS1 cells but not in mouse islets. Collectively, the impaired insulin secretion seen in ATGL-deficient human pseudoislets and INS1 cells cannot be fully accounted for by the decreased activation of MUNC13–1 by reduction of 1-MAG, a mechanism proposed for impaired insulin secretion in MIP-Cre ATGL KO mice (17,38).

ATGL Deficiency Reduces Stx1a Protein in INS1 and Human Islet Cells

As potential targets that explains impaired insulin secretion at exocytosis, expression of SNARE complex proteins was assessed in ATGL-deficient INS1 cells and human pseudoislets. Although synaptosome-associated protein 25 (SNAP25) and MUNC18–1 were not altered, STX1A was significantly reduced in ATGL-deficient human pseudoislets and INS1 cells (Fig. 7*A–F*). *Stx1a* mRNA was not reduced in either INS1 cells or human pseudoislets after ATGL downregulation (Fig. 7*G* and *H*). ATGL was reduced in INS1 cells using a mixture of 15 nmol/L each of two

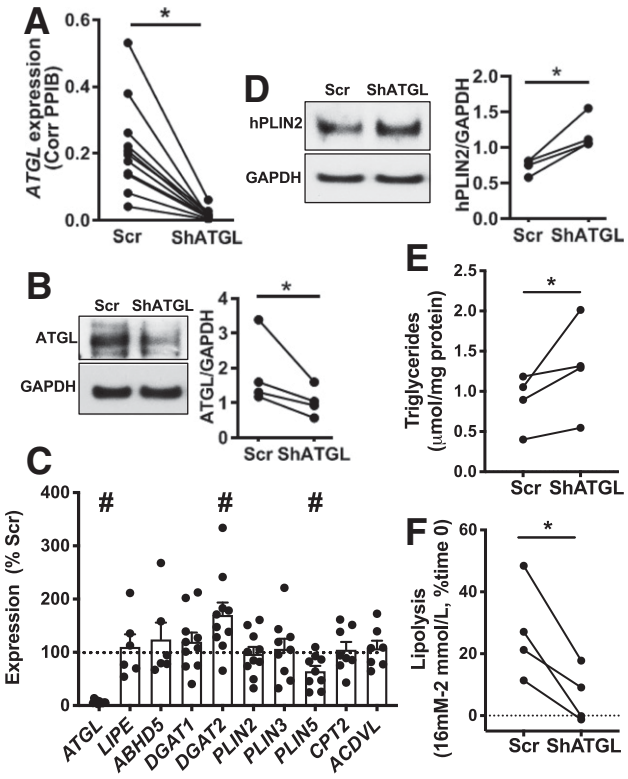

Figure 2—ATGL downregulation in human pseudoislets elevated the levels of PLIN2 without altering genes involved in lipid metabolic and β oxidation. *A*: Expression of *ATGL* in human pseudoislets transduced with lenti-shATGL (shATGL) was compared with those treated with lenti-Sh Scramble (scr) by qPCR. $n = 11$. *B*: An immunoblot comparing ATGL expression in shATGL and scr human pseudoislets. GAPDH served as the loading control, and densitometry data were expressed as ATGL/GAPDH. $n = 4$. *A* and *B*: Each dot represents a single donor, and data points from the same donor are connected by lines. *C*: qPCR probed human pseudoislets for expression levels of genes related to lipid metabolism using PPIB as the internal control. Data are expressed as % scr value. Each dot represents the value for the shATGL islets from one donor. $n = 6$ for *LIPE* and *ABHD5*, $n = 7$ for *ACDVL*, $n = 8$ for *CPT2*, $n = 9$ for *PLIN3* and *PLIN5*, $n = 10$ for *DGAT1*, *DGAT2*, and *PLIN2*, and $n = 11$ donors for *ATGL*. *D*: PLIN2 expression compared between shATGL and scr human pseudoislets by immunoblot as in *B*. $n = 4$. *E*: TG contents of shATGL and scr human pseudoislets. $n = 4$ donors. *F*: The increase in lipolysis in response to glucose measured in shATGL and scr human pseudoislets. Data are expressed taking TG contents per mg protein at time 0 as 100%. $n = 4$ donors. *D–F*: Each dot represents a value from a single donor, and data points from the same donor are connected by lines. All data are mean ± SEM. $^*P < 0.05$, $\#P < 0.05$ vs. scr by Student *t* test.

siRNAs targeting different regions of *Atgl* mRNA (Figs. 5 and 7). To rule out off-target effects, we also downregulated ATGL using each siATGL at 30 nmol/L and confirmed that each siATGL individually reduces GSIS and STX1A protein levels, suggesting that these phenotypes are specific consequences of reduced ATGL expression in INS1 cells (Supplementary Fig. 4*A–D*). In contrast, Stx1a in islets from INS1-Cre ATGL KO mice was not reduced compared with WT (Supplementary Fig. 4*E*) in agreement with the preservation of GSIS in ATGL-deficient mouse islets (Fig. 6*E*). MG132 restored STX1A levels in siATGL INS1 cells indicating that ATGL deficiency accelerates proteasomal degradation of STX1A (Fig. 7*I*). Since lipolytic metabolites, such as FA, may affect protein stability through s-palmitoylation (40), we measured palmitoylation of STX1A using the APEGS assay that differentiates the degree of palmitoylation as mobility shift in immunoblotting (29). As shown in Fig. 7*J*, the ratio of palmitoylated/nonpalmitoylated STX1A was reduced in siATGL INS cells indicating reduced palmitoylation. To confirm that the reduction of STX1A is sufficient to reduce GSIS, *Stx1a* was downregulated using two separate siRNAs each targeting different regions of *Stx1a* (Si1 and Si2) in INS1 cells. STX1A-deficient INS1 cells indeed showed lower GSIS compared with the scr control group for both siRNAs (Fig. 8*A–D*).

DISCUSSION

"Glycerolipid/FA cycle" consisting of TG formation and lipolysis has been proposed to support insulin secretion through the provision of lipolytic metabolites (12). Considering that TG synthesis and lipolysis involve LD formation and mobilization and that LDs are prominent in human β-cells (5,6,9), we sought to understand the regulation of LD turnover in a human β-cell model. We found that ATGL is a key lipase for LD mobilization. The impairment of insulin secretion in ATGL-deficient human pseudoislets was in agreement with previous studies of rodent islets and β-cell lines (15,16,37). However, our study identified the reduction of SNARE protein, STX1A, as a previously unrecognized mechanism. Thus, chronic impairment of LD mobilization impacts β-cell function by a mechanism separate from the proposed acute effect of lipolysis on insulin secretion. Interestingly, glucose increased lipolysis in human islets from donors without diabetes but not in human T2D islets, implicating the dysregulation of lipolysis as a contributing factor for β-cell dysfunction in T2D.

STX1A binds SNAP25 and VAMP-2 to form the SNARE complex that upon protein kinase C–dependent phosphorylation of MUNC18–1 triggers exocytosis (22,41). Although it is debated whether STX1A regulates the first phase or both phases of GSIS (42,43), a key role for STX1A in insulin secretion is well accepted (22,41). The reduced STX1A seen in ATGL-deficient human pseudoislets and INS1 cells may explain the global defect in insulin secretion in these models. In support of this, downregulation of *Stx1a* in INS1 cells impaired GSIS in our study. Interestingly, reduction of SNARE complex proteins including 79% reduction of *Stx1a* was reported in human T2D islets (44). Thus, sustained suppression of lipolysis may impair β-cell function partly by reducing STX1A in T2D.

Independent from a previously reported acute activation of MUNC13–1 by a lipolytic metabolite 1-MAG (17,38), chronic ATGL deficiency appears to impact GSIS by accelerating degradation of STX1A associated with reduced palmitoylation. Also, 1-MAG was not sufficient to rescue

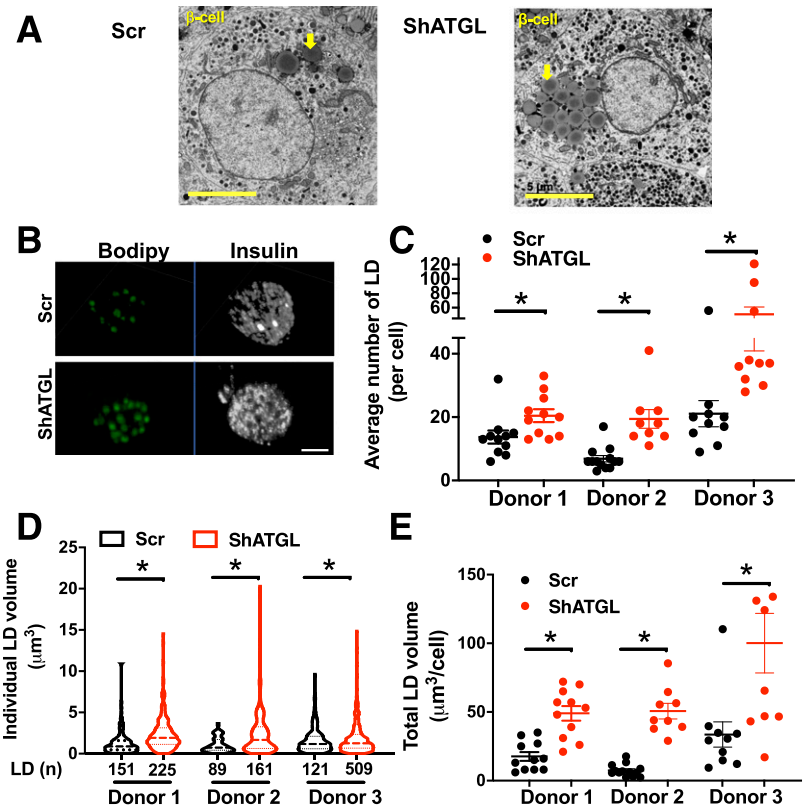

Figure 3—Reduction of ATGL in human pseudoislets increased LD accumulation. *A*: The representative EM images of scr- and shATGL-treated human pseudoislets. Yellow arrows show clusters of LDs. Scale bars = 5 μm. *B*: The representative Z-stack images of β-cells from scr- and shATGL-treated human pseudoislets captured by a confocal microscope. Scale bar = 5 μm. *C–E*: The number of LDs per cell (*C*), the volume distribution of all LDs from all cells within a group (*D*), and the sum of the volume of all LDs in each cell quantitated from the reconstructed three-dimensional images of β-cells from scr and shATGL pseudoislets (*E*). $n = 3$ donors (see Supplementary Table 1 for donor ID). *C* and *E*: The number of cells for donor 1 scr is 11, donor 1 shATGL 11, donor 2 scr 13, donor 2 shATGL 9, donor 3 scr 10, and donor 3 shATGL 10. *D*: The total number of LD for each group is the number of cells counted × number of LD in each cell and shown as LD (*n*) below the *x*-axis. Mean ± SEM is shown. *$P < 0.05$ vs. scr by Student *t* test.

impaired insulin secretion in ATGL-deficient INS1 cells and appeared to have little effect on GSIS of ATGL-deficient human pseudoislets either. *S*-palmitoylation is a highly prevalent posttranslational modification and attaches a long chain FA, predominantly palmitic acid, to cysteine increasing hydrophobicity and affecting stability of proteins in some cases (40,45,46). Although protein acylation has been proposed to mediate lipolytic signaling in β-cells (10,47), our study demonstrates lipolysis-dependent palmitoylation in a protein that directly regulates insulin secretion. Further studies are required to confirm whether the reduced palmitoylation is sufficient to accelerate degradation of STX1A in β-cells and how lipolytic signal(s) select target proteins. Notably, palmitoylation is known to be required for membrane association of SNAP25 (48), but SNAP25 expression was not reduced in our study.

The marked increase in LDs in ATGL-deficient human β-cells confirms that LD represents a dynamic organelle whose mobilization is regulated by ATGL in human β-cells. It was reported that human but not mouse islets transplanted into immunodeficient mice increased LDs in response to HFD (6). Collectively, the dynamic formation of LD is a feature of human β-cells not shared with mouse islets despite TG accumulation upon lipid load being reported in mouse β-cells (5,7). Although it is premature to conclude that size of LDs affects lipolysis, significant dissimilarities in glucose-responsive lipolysis and the impact of ATGL deficiency on GSIS were noted between Bl6 and human islets. As LDs are demonstrable in rat β-cells (30,49) and INS1 cells, the lack of visible LDs is not a universal feature of rodent β-cells. Interestingly, INS1 cells, like human β-cells, increased lipolysis by glucose and decreased GSIS and STX1A after ATGL downregulation. Overall, it seems that the regulation of lipolysis relevant to the pathophysiology of human β-cells is better studied in a model that captures features of human β-cells. This is a significant point considering the increase in lipid accumulation in human T2D islets (8,9) and dysregulation of lipolysis in T2D. Hence, LDs in β-cells represent a highly relevant organelle in the pathogenesis of T2D.

ATGL mutations in humans cause neutral lipid storage disease with myopathy, a disease with progressive muscle dystrophy and heart failure (50,51). An increased susceptibility to T2D is also noted in neutral lipid storage disease

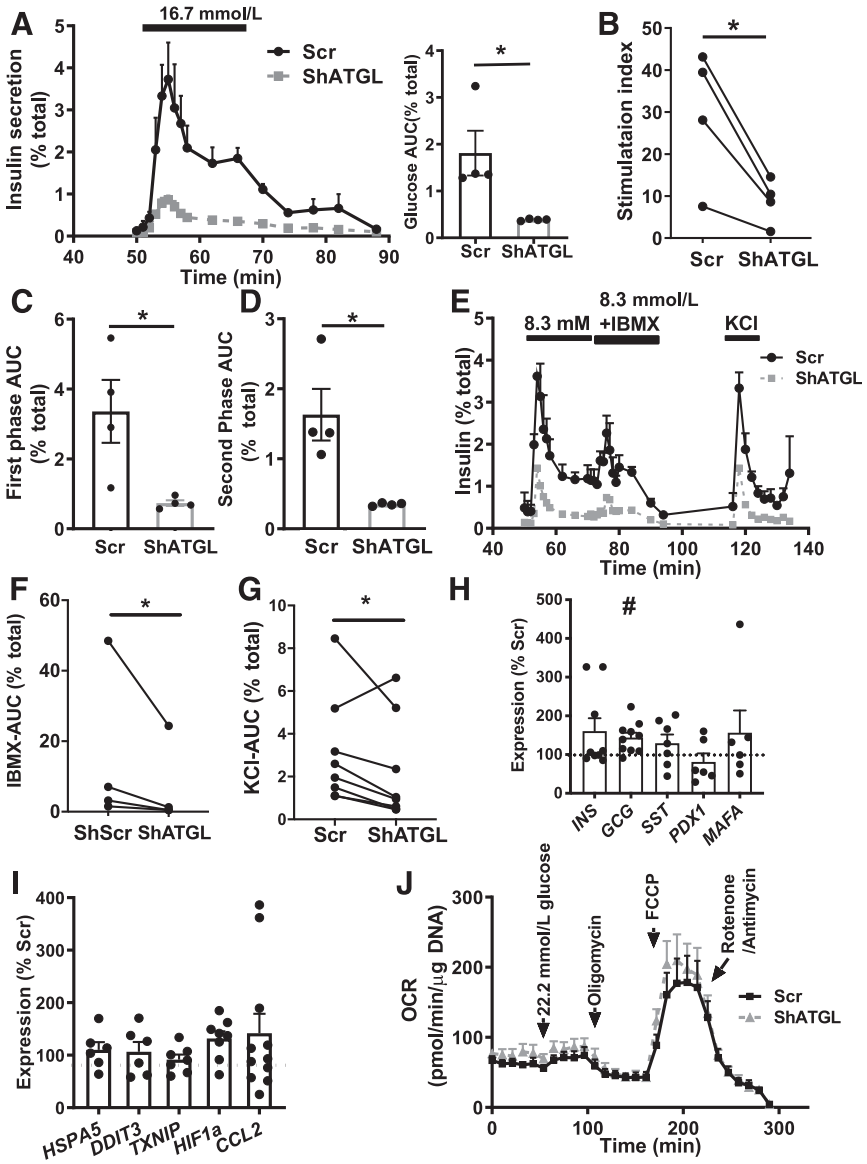

Figure 4—Insulin secretion was impaired in human pseudoislets transduced with shATGL. *A*: Perifusion profile of GSIS from pseudoislets transduced by lenti-shATGL (shATGL) and those transduced by lenti-shScr (scr) in response to 16.7 mmol/L glucose expressed as % of total insulin. The glucose ramp is indicated in a bar on the top. The line graph was analyzed by two-way ANOVA, $P < 0.05$. AUC during the glucose ramp is also shown. $n = 4$ donors. *B*: SI of GSIS in *A*. Each dot represents a single donor and data from the same donor are connected by lines. *C* and *D*: AUC during the first phase (*C*) and the second phase (*D*) of GSIS during glucose ramp in *A*. *E*: Representative profile of insulin secretion from scr and shATGL human pseudoislets sequentially perifused with 8.3 mmol/L glucose, 8.3 mmol/L glucose + 0.1 mmol/L IBMX, and 30 mmol/L KCl expressed as % of total insulin. Mean ± SEM of duplicates from a single donor. AUC for IBMX treatment (*F*) ($n = 5$) and for KCl treatment (*G*) ($n = 7$) during glucose ramp in *E*. For *A–D*, data represent mean ± SEM. *$P < 0.05$ vs. scr by Student *t* test. *H* and *I*: qPCR probed human pseudoislets for expression levels of genes related to endocrine cell types (*H*) and stress markers (*I*) using PPIB as internal control. Data are expressed as % scr. Each dot represents value for shATGL islets from one donor. Data are mean ± SEM. $n = 6$ for *PDX1*, *MAFA*, *HSPA5*, and *DDIT3*; $n = 7$ for *SST*, *TXNIP*, and *HIF1a*; $n = 9$ for *INS*; $n = 10$ for *GCG*; and $n = 11$ donors for *CCL2*. *$P < 0.05$. #$P < 0.05$ vs. scr by Student *t* test. *J*: Sequential change in OCR in response to 22.2 mmol/L glucose, oligomycin, FCCP, and rotenone + antimycin are compared between scr and shATGL pseudoislets. Data are corrected for DNA contents and mean ± SEM, $n = 4$. Data are representative of experiments repeated in three donors.

with myopathy (50), in which case islet ATGL may directly contribute based on observations of islet dysfunction in ATGL-deficient human pseudoislets (50). As PPARα activation by an agonist was sufficient to improve TG accumulation and cardiac function in ATGL-deficient heart in mice, generation of FA as a signaling molecule is considered to be a key factor by which ATGL regulates lipid accumulation in the heart, at least in mice (51,52). Interestingly, blunted activation of the FA target, PPARδ, and subsequent mitochondrial dysfunction were noted in islets of RIP-Cre ATGL KO mice on HFD (15). However, our current study and a previous study of MIP-Cre ATGL

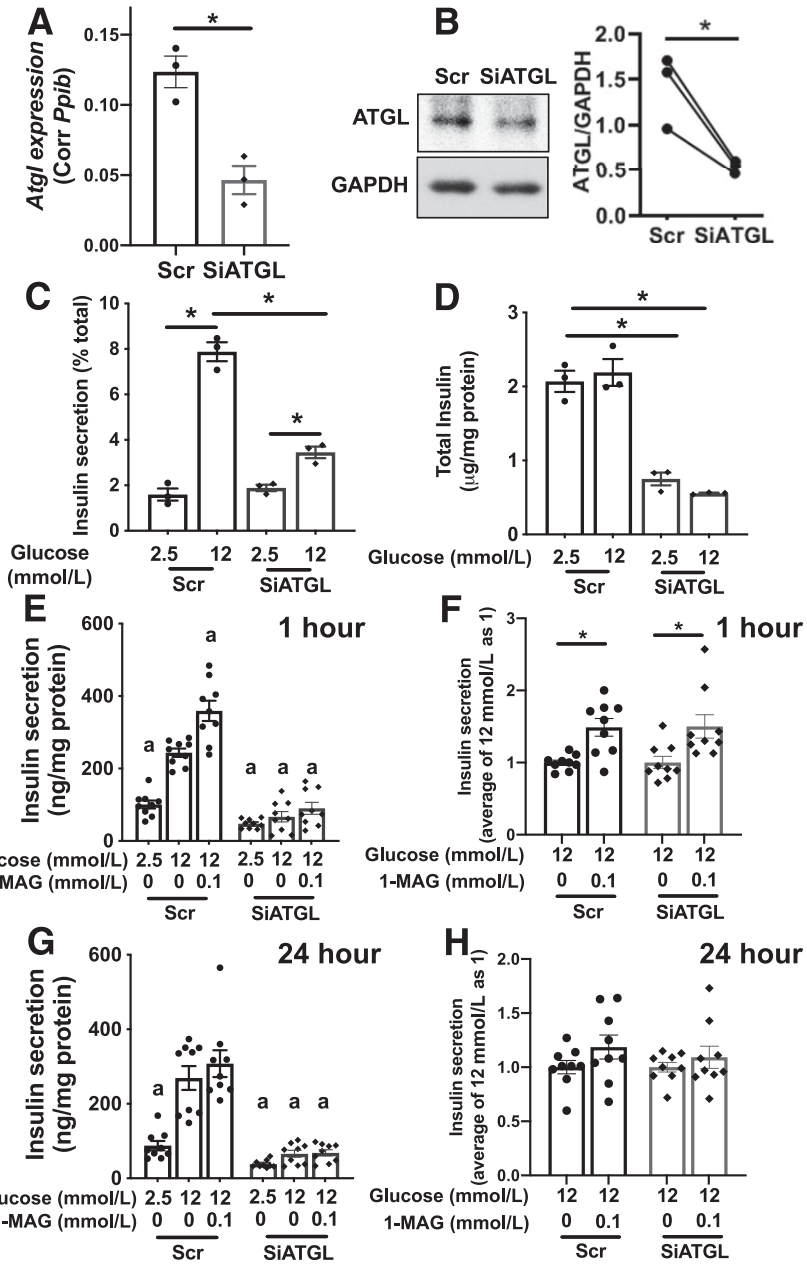

Figure 5—ATGL reduction impaired GSIS in INS1 cells that was not fully restored by addition of 1-palmitoyl-glycerol. *A–H*: ATGL was downregulated in INS1 cells by SiATGL (15 nmol/L each of rn.Ri.Pnpla2.13.2 and rn.Ri.Pnpla2.13.3 combined) using 30 nmol/L of nontargeting RNA (scr) as a control. *A*: qPCR compared *Atgl* mRNA expression between scr- and SiATGL-treated INS1 cells. *B*: Representative immunoblot and densitometry analysis of ATGL/GAPDH. Data from paired samples are connected by lines. $n = 3$. *C*: Insulin secretion measured by static incubation at indicated concentration of glucose in SiATGL INS1 cells and the scr control group. *D*: Total insulin contents corrected for protein. *A*, *C*, and *D*: $n = 3$, representative of six experiments. *A–D*: $^*P < 0.05$ by Student *t* test. *E–H*: Insulin secretion as measured by static incubation at indicated concentration of glucose with or without 0.1 mmol/L 1-palmitoyl-glycerol (1-MAG) for 1 h (*E* and *F*) or 24 h (*G* and *H*) in INS1 cells treated with siATGL and the scr control group. *E* and *G*: Data are expressed per protein contents and combine three experiments each performed in triplicates. $n = 9$. $^aP < 0.05$ vs. scr 12 mmol/L glucose by one-way ANOVA with Dunnett multiple comparisons test. *F*: Fold increase of insulin secretion in (*E*, 1 h 1-MAG treatment) and (*H*) fold increase of insulin secretion in (*G*, 24 h 1-MAG treatment) taking average insulin secretion at 12 mmol/L glucose as 1. $n = 9$. *F* and *H*: $^*P < 0.05$ for data ± 1-MAG by Student *t* test. All data represent mean ± SEM.

KO mice (16) showed that ATGL deficiency in β-cells impairs GSIS without mitochondrial dysfunction evidenced by normal OCR and normal expression of PPARδ target genes. In MIP-Cre ATGL KO mice, lower insulin secretion is attributed to reduced production of 1-MAG, but it can partly be affected by improved insulin sensitivity in this model (16). In our study of young INS1-Cre ATGL KO mice on regular chow, there was not clear reduction of GSIS to the extent seen in ATGL-deficient human pseudoislets and INS1 cells despite marked reduction of ATGL

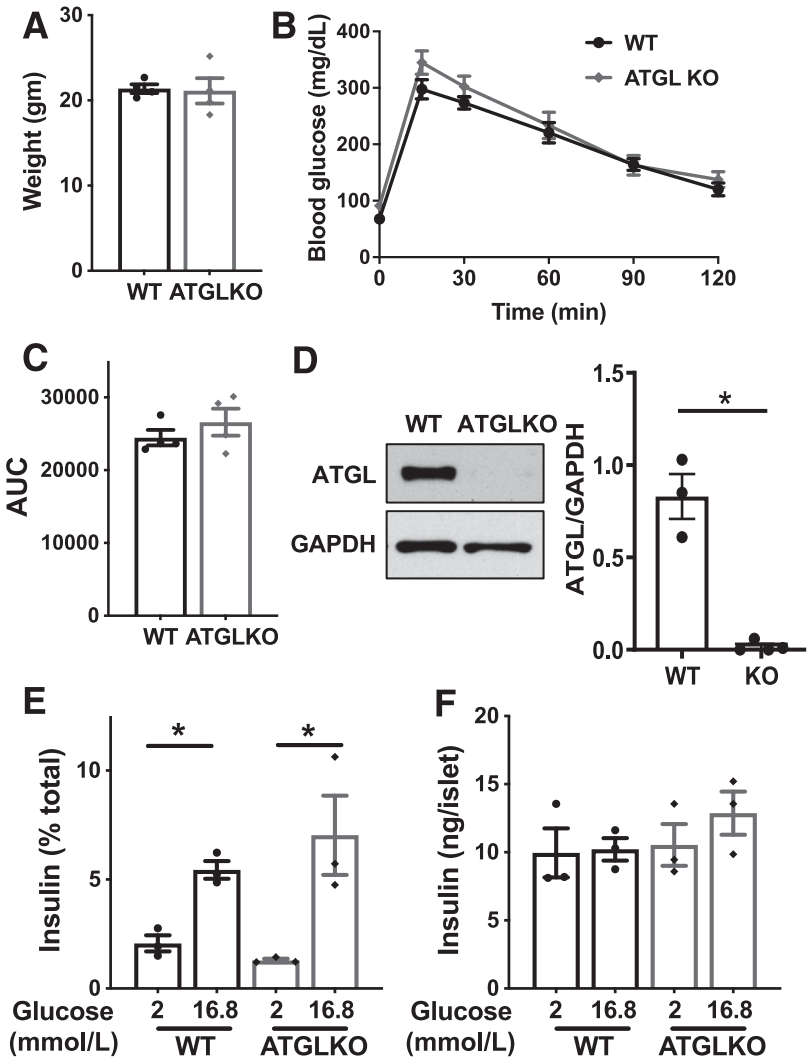

Figure 6—ATGL reduction is not sufficient to impair GSIS in mouse islets. *A–C*: Body weight (*A*), tail blood glucose (*B*), and area under curve (AUC) (*C*) are compared between 2-month-old male ATGL KO mice and WT littermates. $P = 0.22$ by two-way ANOVA for *B*. $n = 4$ per group. *D*: Immunoblot compared ATGL and GAPDH expression in islets from β-cell–specific ATGL KO mice and WT littermates. A represenative blot and densitometry data of ATGL/GAPDH. $n = 3$ for WT and 4 for KO. *E* and *F*: GSIS measured by static incbuation corrected for insulin contents (*E*) and total insulin content (*F*) in WT and ATGL KO mouse islets. Representative of experiments performed in six mice total for WT and ATGL KO. Each data points represent the average of triplicates from one mouse. $n = 3$ mice. All data represent mean ± SEM. *$P < 0.05$ by Student *t* test.

in islets. Species, genetic background, Cre models, dietary FA load, housing environment including gut microbiota, and age could all potentially contribute to the absence and presence of mitochondrial changes and secretory defects among three different mouse models of β-cell–specific ATGL KO. Further study is required to test whether the prolonged downregulation of ATGL or exposure to FA causes mitochondrial dysfunction in human islets as was seen in RIP-Cre ATGL KO mice on HFD (15).

Although phosphorylation of PLIN1 by protein kinase A is a well-characterized trigger of lipolysis in adipocytes (11,53), regulation of lipolysis in nonadipocytes remains undefined (11,53). ATGL phosphorylation, association between ATGL and colipases, and profiles of PLIN on the surface of LD are proposed to modulate lipolysis in nonadipocytes that express little PLIN1 (11,51,53,54). As PLIN1 overexpression in INS1 cells reduced lipolysis (55) and PLIN5 overexpression in MIN6 cells increased basal and cAMP stimulated lipolysis (5), each PLIN likely affects lipolysis differently in β-cells. However, further studies are needed to determine whether PLINs or other factors mediate the upregulation of lipolysis by glucose in β-cells, an issue critical to understanding the mechanism by which glucose-stimulated lipolysis is impaired in T2D islets. Of note, dysregulation of lipolysis in T2D islets cannot be attributed to the reduction in ATGL based on our Western blot and single-cell RNA sequencing data that did not identify *ATGL* as T2D-associated genes (56).

The difficulty in demonstrating LDs in mouse β-cells is puzzling because they express key genes for TG synthesis

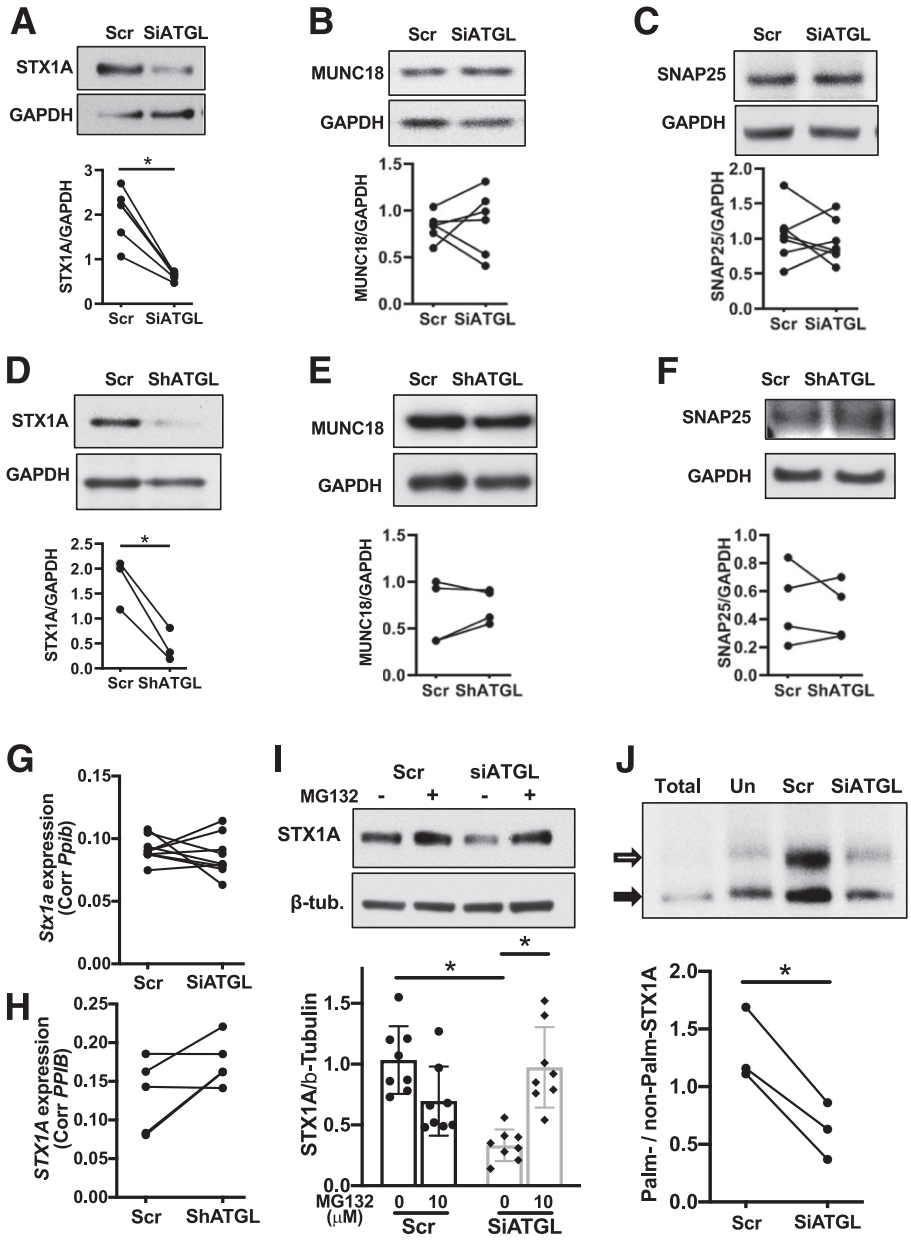

Figure 7—The downregulation of ATGL decreased the levels of Stx1a in INS1 and human islets. *A–C*: Immunoblot probed INS1 cells treated with siATGL (15 nmol/L each of rn.Ri.Pnpla2.13.2 and rn.Ri.Pnpla2.13.3 combined) and 30 nmol/L of scr control for STX1A (*A*), MUNC18–1 (MUNC18) (*B*), and SNAP25 (*C*). Representative blot from four experiments. Densitometry data from the paired samples are connected by lines. *D–F*: Immunoblot probed human pseudoislets treated with shATGL and scr control for STX1A (*D*), MUNC18 (*E*), and SNAP25 (*F*). Representative blot from $n = 4$ donors. Each dot represents densitometry data from each donor and data from the same donor are connected by lines. Bar graphs indicate mean ± SEM of the densitometry data. *G* and *H*: *Stx1a* mRNA levels compared between INS1 cells treated with siATGL (15 nmol/L each of rn.Ri.Pnpla2.13.2 and rn.Ri.Pnpla2.13.3 combined) and 30 nmol/L of scr control. $n = 6$ (*G*) and between control and ATGL silenced human pseudoislets, $n = 4$ (*H*). *I*: Immunoblot of STX1A and β-tubulin (β-tub) in scr and siATGL INS1 cells (15 nmol/L each of rn.Ri.Pnpla2.13.2 and rn.Ri.Pnpla2.13.3 combined) treated with or without 100 μmol/L MG132 for 8 h prior to harvest. Representative blot and densitometry data taking average for scr without MG132 as 1. Mean ± SEM. $n = 8$ for without MG132, and $n = 10$ for with MG132. *J*: APEGS assay of STX1A comparing protein lysate from INS1 cells treated with 15 nmol/L each of rn.Ri.Pnpla2.13.2 and rn.Ri.Pnpla2.13.3 combined (Si) and 30 nmol/L of the scr control group. Protein lysate untreated with hydroxylamine is the negative control (Un). A representative Western blot from three independent experiments and densitometry data are shown. The black arrow shows a nonpalmitoylated band, and the white arrow shows a palmitoylated band. *$P < 0.05$ by Student *t* test.

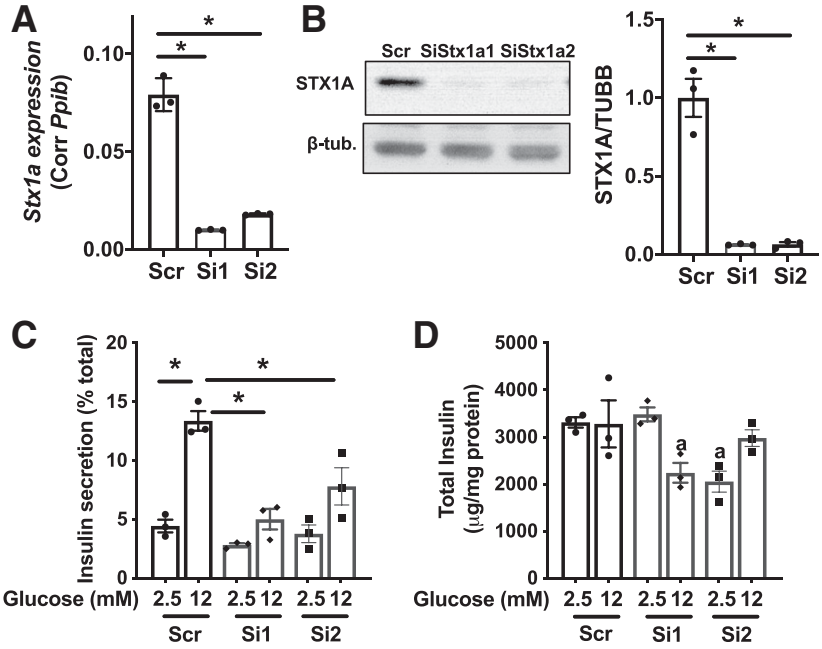

Figure 8—The downregulation of Stx1a decreased GSIS in INS1 cells. *A*: qPCR compared *Stx1a* mRNA expression corrected for *Ppib* in INS1 cells. The scr control group is compared with cells treated with two separate SiStx1a (1,2). *B*: Immunoblot probed STX1A in INS1 cells treated with two separate SiStx1a and scr control. Representative blot and densitometry data from three experiments each performed in triplicates. *C*: Insulin secretion measured by static incubation expressed per total insulin content. *D*: The total insulin content for data in *C* corrected for protein. Representative data from three experiments each performed in triplicates. All data are mean ± SEM. $^*P < 0.05$ by one-way ANOVA with Dunnett multiple comparisons test.

(*Dgat1* and *Dgat2*), LD formation (*Plin2*, *Plin3*, and *Plin5*), and lipolysis (*Atgl*, *Lipe*, and *Abhd5*) (5,7). Deep sequencing data of purified β-cells reports similar expression of *Atgl*, *Dgat1*, *Plin2*, and *Abhd5* between human and mouse β-cells, while *Plin3* is higher in human and *Lipe* is higher in mouse β-cells (57). It will require further studies to determine whether the differential expression of *Plin3* or *Lipe* translates into differences in protein levels and altered kinetics of LD formation and mobilization between human and mouse β-cells. Considering relatively high basal lipolysis at low glucose in mouse islets, LDs in mouse β-cells may be rapidly mobilized before expanding size.

We measured lipolysis as the reduction of TG in the presence of triacsin C to inhibit TG synthesis (24) since glycerol is reported to be an inaccurate measure of lipolysis in β-cells (21). We observed that glucose mobilizes >30% of TG in human pseudoislets and INS1 cells over 90 min revealing highly dynamic turnover of LDs. To complete the picture of LD turnover, it is important to recognize that TG is constantly added to LDs by TG synthesis, a process also upregulated by glucose at a rate likely higher than lipolysis, thereby, expanding the total TG pool under high glucose (10). This seemingly futile glycerolipid/FA cycle may allow distribution of lipolytic metabolites to a specific intracellular component through the mobility of LDs and contribute to the stability of STX1A through protein palmitoylation. It also needs to be noted that our lipolysis measurement did not assess total lipolytic metabolites. Considering that the rate of lipolysis is markedly blunted, we estimate that an approximately twofold increase in TG would not be sufficient to maintain the production of lipolytic metabolites in T2D islets. However, it warrants metabolome-based quantification of lipolytic metabolites between islets from donors without diabetes and those from donors with T2D to draw conclusions regarding the impact of dysregulated lipolysis on total metabolite production in T2D islets.

Our studies have several limitations. We have previously shown that human pseudoislets maintain features of original intact human islets over time (27). However, this cultured islet model might not fully recapitulate all features of human islets in vivo. Also, ATGL was downregulated in both non-β-cells and β-cells in human pseudoislets (58). While the imaging study selectively monitored β-cells, the change in GSIS may reflect the impact of ATGL downregulation in β-cells and non-β-cells. qPCR data showed an increase in *GCG* without change in *INS* in shATGL pseudoislets (Fig. 4*H*). Although we did not see decreases in other β-cell markers (Fig. 4*H*) or increases in stress markers (Fig. 4*I*) with shATGL treatment, we cannot rule out selective loss of insulin-positive cells, increased α cell proliferation, and/or transdifferentiation of insulin-positive cells to glucagon-positive cells in ATGL-deficient human pseudoislets; considering that α cells also express ATGL at comparable level as β-cells (56,57). However, our preliminary data showed that LDs are richer in β-cells than α cells, the second most abundant cells in human islets. Also,

we have utilized INS1 cells to supplement findings in human islets. To ensure the specificity of siRNA/shRNA, we tested two independent siRNAs/shRNAs that target different regions of ATGL and STX1A. However, re-expression of ATGL and STX1A to rescue the phenotype would be needed to further confirm the specificity of phenotypes. While ATGL deficiency reduced insulin secretion and STX1A in both human pseudoislets and INS1 cells, INS1 cells differ from human pseudoislets in the reduction of total insulin by siATGL. As insulin secretion was lower in ATGL-deficient INS1 cells even after correction for total insulin, lowering of total insulin in INS1 cells does not change our interpretation. However, we do not have an explanation why ATGL deficiency in INS1 cells reduced insulin content. One possibility is that change in insulin secretion secondarily affects total insulin content in INS1 cells but not in human pseudoislets. We have observed a correlation between insulin secretion and total insulin when other targets were manipulated in INS1 cells. Total insulin content increases when PLIN2 downregulation increases insulin secretion (Y.I., unpublished data) and total insulin contents decrease when STX1A (Fig. 8) and DHHC1 (Y.I., unpublished data) reduce insulin secretion in INS1 cells.

In summary, ATGL is a principle lipase in human β-cells and is indispensable for normal insulin secretion in human pseudoislets. STX1A is a previously unrecognized target of ATGL in supporting insulin secretion by human pseudoislets and INS1 cells. Interestingly, human islets from T2D donors showed dysregulation in lipolysis indicating a potential contribution of lipolysis to the β-cell dysfunction in T2D.

Acknowledgments. The authors thank Assistant Director Dr. Thomas Moninger at the Central Microscopy Research Facility (CMRF), University of Iowa, Iowa City, IA, for technical assistance.

Funding. E.B.T. is supported by National Institute of Diabetes and Digestive and Kidney Diseases (R01-DK-104998). A.J.B. is supported by a National Institute of Neurological Disorders and Stroke training grant (T32NS45549). J.A.A. is supported by the Fraternal Order of Eagles Diabetes Research Center. This work was financially supported by National Institute of Diabetes and Digestive and Kidney Diseases grant R01-DK-090490 and American Diabetes Association grant 1-17-IBS-132 (both to Y.I.). The authors used human pancreatic islets provided by the National Institute of Diabetes and Digestive and Kidney Diseases, Integrated Islet Distribution Program at City of Hope (2UC4-DK-098085). A Zeiss LSM710 confocal microscope (1 S10 RR025439-01) and a JEOL JEM-1230 transmission electron microscope (1 S10 RR018998-01) located in the CMRF were purchased through the indicated National Institutes of Health Shared Instrument Grant. Parts of this study were supported by resources and the use of facilities at the Department of Veterans Affairs Health Care System, Iowa City, IA.

Duality of Interest. No potential conflicts of interest relevant to this article were reported.

Author Contributions. S.L. contributed to all aspects of the data acquisition and analysis. S.L. and Y.I. contributed to research design. S.L., J.A.P., and Y.I. contributed to interpretation of the data, drafted the manuscript, and critically revised the manuscript for important intellectual content. J.A.P. and S.B.S. contributed to the data acquisition and analysis for the INS1 cell studies. M.H. contributed to the data acquisition and analysis for the lentivirus production and human pseudoislet studies. A.M., W.I.S., and B.D.F. contributed to the data acquisition and analysis for the Seahorse metabolic analyzer. E.B.T. contributed to the data acquisition and analysis for the lipolysis assay. A.J.B. and J.A.A. contributed to the data acquisition and analysis for the islet size acquisition. Y.I. conceived the study and is responsible for all contents of the manuscript. All authors revised and approved the final version of the manuscript. Y.I. is the guarantor of this work and, as such, had full access to all the data in the study and takes responsibility for the integrity of the data and the accuracy of the data analysis.

Prior Presentation. Parts of this study were presented at Midwest Islet Club, University of Michigan, Ann Arbor, MI, 19–20 May 2019.

References

1. Samuel VT, Shulman GI. The pathogenesis of insulin resistance: integrating signaling pathways and substrate flux. J Clin Invest 2016;126:12–22

2. Shimabukuro M, Zhou YT, Levi M, Unger RH. Fatty acid-induced beta cell apoptosis: a link between obesity and diabetes. Proc Natl Acad Sci U S A 1998;95:2498–2502

3. Kahn SE, Cooper ME, Del Prato S. Pathophysiology and treatment of type 2 diabetes: perspectives on the past, present, and future. Lancet 2014;383:1068–1083

4. Greenberg AS, Coleman RA, Kraemer FB, et al. The role of lipid droplets in metabolic disease in rodents and humans. J Clin Invest 2011;121:2102–2110

5. Trevino MB, Machida Y, Hallinger DR, et al. Perilipin 5 regulates islet lipid metabolism and insulin secretion in a cAMP-dependent manner: implication of its role in the postprandial insulin secretion. Diabetes 2015;64:1299–1310

6. Dai C, Kayton NS, Shostak A, et al. Stress-impaired transcription factor expression and insulin secretion in transplanted human islets. J Clin Invest 2016;126:1857–1870

7. Faleck DM, Ali K, Roat R, et al. Adipose differentiation-related protein regulates lipids and insulin in pancreatic islets. Am J Physiol Endocrinol Metab 2010;299:E249–E257

8. Ji J, Petropavlovskaia M, Khatchadourian A, et al. Type 2 diabetes is associated with suppression of autophagy and lipid accumulation in β-cells. J Cell Mol Med 2019;23:2890–2900

9. Tong X, Dai C, Walker JT, et al. Lipid droplet accumulation in human pancreatic islets is dependent on both donor age and health. Diabetes 2020;69:342–354

10. Imai Y, Cousins RS, Liu S, Phelps BM, Promes JA. Connecting pancreatic islet lipid metabolism with insulin secretion and the development of type 2 diabetes. Ann N Y Acad Sci 2020;1461:53–72

11. Zechner R, Madeo F, Kratky D. Cytosolic lipolysis and lipophagy: two sides of the same coin. Nat Rev Mol Cell Biol 2017;18:671–684

12. Prentki M, Madiraju SR. Glycerolipid/free fatty acid cycle and islet β-cell function in health, obesity and diabetes. Mol Cell Endocrinol 2012;353:88–100

13. Corkey BE, Deeney JT, Yaney GC, Tornheim K, Prentki M. The role of long-chain fatty acyl-CoA esters in beta-cell signal transduction. J Nutr 2000;130(Suppl.):299S–304S

14. Fex M, Mulder H. Lipases in the pancreatic beta-cell: implications for insulin secretion. Biochem Soc Trans 2008;36:885–890

15. Tang T, Abbott MJ, Ahmadian M, Lopes AB, Wang Y, Sul HS. Desnutrin/ATGL activates PPARδ to promote mitochondrial function for insulin secretion in islet β cells. Cell Metab 2013;18:883–895

16. Attané C, Peyot ML, Lussier R, et al. A beta cell ATGL-lipolysis/adipose tissue axis controls energy homeostasis and body weight via insulin secretion in mice. Diabetologia 2016;59:2654–2663

17. Zhao S, Mugabo Y, Iglesias J, et al. α/β-Hydrolase domain-6-accessible monoacylglycerol controls glucose-stimulated insulin secretion. Cell Metab 2014;19:993–1007

18. Berdan CA, Erion KA, Burritt NE, Corkey BE, Deeney JT. Inhibition of monoacylglycerol lipase activity decreases glucose-stimulated insulin secretion in INS-1 (832/13) cells and rat islets. PLoS One 2016;11:e0149008

19. Peyot ML, Nolan CJ, Soni K, et al. Hormone-sensitive lipase has a role in lipid signaling for insulin secretion but is nonessential for the incretin action of glucagon-like peptide 1. Diabetes 2004;53:1733–1742
20. Nolan CJ, Leahy JL, Delghingaro-Augusto V, et al. Beta cell compensation for insulin resistance in Zucker fatty rats: increased lipolysis and fatty acid signalling. Diabetologia 2006;49:2120–2130
21. Mugabo Y, Zhao S, Seifried A, et al. Identification of a mammalian glycerol-3-phosphate phosphatase: role in metabolism and signaling in pancreatic β-cells and hepatocytes. Proc Natl Acad Sci U S A 2016;113:E430–E439
22. Gaisano HY. Recent new insights into the role of SNARE and associated proteins in insulin granule exocytosis. Diabetes Obes Metab 2017;19(Suppl. 1): 115–123
23. Bearrows SC, Bauchle CJ, Becker M, Haldeman JM, Swaminathan S, Stephens SB. Chromogranin B regulates early-stage insulin granule trafficking from the Golgi in pancreatic islet β-cells. J Cell Sci 2019;132:jcs231373
24. Paar M, Jüngst C, Steiner NA, et al. Remodeling of lipid droplets during lipolysis and growth in adipocytes. J Biol Chem 2012;287:11164–11173
25. Liu S, Harata M, Promes JA, Burand AJ, Ankrum JA, Imai Y. Lentiviral mediated gene silencing in human pseudoislet prepared in low attachment plates. J Vis Exp 2019;147
26. Livak KJ, Schmittgen TD. Analysis of relative gene expression data using real-time quantitative PCR and the 2(-Delta Delta C(T)) method. Methods 2001;25: 402–408
27. Harata M, Liu S, Promes JA, Burand AJ, Ankrum JA, Imai Y. Delivery of shRNA via lentivirus in human pseudoislets provides a model to test dynamic regulation of insulin secretion and gene function in human islets. Physiol Rep 2018;6:e13907
28. Imai Y, Fink BD, Promes JA, Kulkarni CA, Kerns RJ, Sivitz WI. Effect of a mitochondrial-targeted coenzyme Q analog on pancreatic β-cell function and energetics in high fat fed obese mice. Pharmacol Res Perspect 2018;6:e00393
29. Kanadome T, Yokoi N, Fukata Y, Fukata M. Systematic screening of depalmitoylating enzymes and evaluation of their activities by the acyl-PEGyl exchange gel-shift (APEGS) assay. Methods Mol Biol 2019;2009:83–98
30. Vernier S, Chiu A, Schober J, et al. β-cell metabolic alterations under chronic nutrient overload in rat and human islets. Islets 2012;4:379–392
31. Quinlivan VH, Wilson MH, Ruzicka J, Farber SA. An HPLC-CAD/fluorescence lipidomics platform using fluorescent fatty acids as metabolic tracers. J Lipid Res 2017;58:1008–1020
32. Mayer N, Schweiger M, Romauch M, et al. Development of small-molecule inhibitors targeting adipose triglyceride lipase. Nat Chem Biol 2013;9:785–787
33. Iglesias J, Lamontagne J, Erb H, et al. Simplified assays of lipolysis enzymes for drug discovery and specificity assessment of known inhibitors. J Lipid Res 2016;57:131–141
34. Buckley D, Duke G, Heuer TS, et al. Fatty acid synthase - modern tumor cell biology insights into a classical oncology target. Pharmacol Ther 2017;177:23–31
35. Zuellig RA, Cavallari G, Gerber P, et al. Improved physiological properties of gravity-enforced reassembled rat and human pancreatic pseudo-islets. J Tissue Eng Regen Med 2017;11:109–120
36. Xu G, Sztalryd C, Lu X, et al. Post-translational regulation of adipose differentiation-related protein by the ubiquitin/proteasome pathway. J Biol Chem 2005;280:42841–42847
37. Peyot ML, Guay C, Latour MG, et al. Adipose triglyceride lipase is implicated in fuel- and non-fuel-stimulated insulin secretion. J Biol Chem 2009;284:16848–16859
38. Zhao S, Poursharifi P, Mugabo Y, et al. α/β-Hydrolase domain-6 and saturated long chain monoacylglycerol regulate insulin secretion promoted by both fuel and non-fuel stimuli. Mol Metab 2015;4:940–950
39. Thorens B, Tarussio D, Maestro MA, Rovira M, Heikkilä E, Ferrer J. Ins1(Cre) knock-in mice for beta cell-specific gene recombination. Diabetologia 2015;58: 558–565
40. Jiang H, Zhang X, Chen X, Aramsangtienchai P, Tong Z, Lin H. Protein lipidation: occurrence, mechanisms, biological functions, and enabling technologies. Chem Rev 2018;118:919–988
41. Wang Z, Thurmond DC. Mechanisms of biphasic insulin-granule exocytosis - roles of the cytoskeleton, small GTPases and SNARE proteins. J Cell Sci 2009;122: 893–903
42. Liang T, Qin T, Xie L, et al. New roles of syntaxin-1A in insulin granule exocytosis and replenishment. J Biol Chem 2017;292:2203–2216
43. Ohara-Imaizumi M, Fujiwara T, Nakamichi Y, et al. Imaging analysis reveals mechanistic differences between first- and second-phase insulin exocytosis. J Cell Biol 2007;177:695–705
44. Ostenson CG, Gaisano H, Sheu L, Tibell A, Bartfai T. Impaired gene and protein expression of exocytotic soluble N-ethylmaleimide attachment protein receptor complex proteins in pancreatic islets of type 2 diabetic patients. Diabetes 2006;55:435–440
45. Ampah KK, Greaves J, Shun-Shion AS, et al. S-acylation regulates the trafficking and stability of the unconventional Q-SNARE STX19. J Cell Sci 2018;131
46. Lanyon-Hogg T, Faronato M, Serwa RA, Tate EW. Dynamic protein acylation: new substrates, mechanisms, and drug targets. Trends Biochem Sci 2017;42:566–581
47. Yaney GC, Corkey BE. Fatty acid metabolism and insulin secretion in pancreatic beta cells. Diabetologia 2003;46:1297–1312
48. Gonelle-Gispert C, Molinete M, Halban PA, Sadoul K. Membrane localization and biological activity of SNAP-25 cysteine mutants in insulin-secreting cells. J Cell Sci 2000;113:3197–3205
49. Man ZW, Zhu M, Noma Y, et al. Impaired beta-cell function and deposition of fat droplets in the pancreas as a consequence of hypertriglyceridemia in OLETF rat, a model of spontaneous NIDDM. Diabetes 1997;46:1718–1724
50. Missaglia S, Coleman RA, Mordente A, Tavian D. Neutral lipid storage diseases as cellular model to study lipid droplet function. Cells 2019;8:E187
51. Schreiber R, Xie H, Schweiger M. Of mice and men: the physiological role of adipose triglyceride lipase (ATGL). Biochim Biophys Acta Mol Cell Biol Lipids 2019; 1864:880–899
52. Haemmerle G, Moustafa T, Woelkart G, et al. ATGL-mediated fat catabolism regulates cardiac mitochondrial function via PPAR-α and PGC-1. Nat Med 2011; 17:1076–1085
53. Sztalryd C, Brasaemle DL. The perilipin family of lipid droplet proteins: gatekeepers of intracellular lipolysis. Biochim Biophys Acta Mol Cell Biol Lipids 2017;1862:1221–1232
54. Pagnon J, Matzaris M, Stark R, et al. Identification and functional characterization of protein kinase A phosphorylation sites in the major lipolytic protein, adipose triglyceride lipase. Endocrinology 2012;153:4278–4289
55. Borg J, Klint C, Wierup N, et al. Perilipin is present in islets of Langerhans and protects against lipotoxicity when overexpressed in the beta-cell line INS-1. Endocrinology 2009;150:3049–3057
56. Xin Y, Kim J, Okamoto H, et al. RNA sequencing of single human islet cells reveals type 2 diabetes genes. Cell Metab 2016;24:608–615
57. Benner C, van der Meulen T, Cacéres E, Tigyi K, Donaldson CJ, Huising MO. The transcriptional landscape of mouse beta cells compared to human beta cells reveals notable species differences in long non-coding RNA and protein-coding gene expression. BMC Genomics 2014;15:620
58. Arrojo e Drigo R, Ali Y, Diez J, Srinivasan DK, Berggren PO, Boehm BO. New insights into the architecture of the islet of Langerhans: a focused cross-species assessment. Diabetologia 2015;58:2218–2228